ADSORPTION EQUILIBRIUM AND KINETICS STUDIES OF DIVALENT MANGANESE FROM PHOSPHORIC ACID SOLUTION BY USING CATIONIC EXCHANGE RESIN

[1]Haydarov Bekzod, [2]Asamov Javlon, [3]Mansurov Tolmos, [4]Eshmurzayev Qurbonmurot, [5]Qudratova Iroda

[1,2]Assistant teachers of Yangiyer branch of Tashkent Institute of Chemical Technology
[3]Senior teacher of Yangiyer branch of Tashkent Institute of Chemical Technology
[4,5]Students of Yangiyer branch of Tashkent Institute of Chemical Technology

https://doi.org/10.5281/zenodo.8044425

Abstract. *There are numerous impurities in wet-process phosphoric acid, among which manganese is one of detrimental metallic impurities, and it causes striking negative effects on the industrial phosphoric acid production and downstream commodity. This article investigated the adsorption behavior of manganese from phosphoric acid employing Sinco-430 cationic ion-exchange resin. Resorting FT-IR and XPS characterizations, the adsorption mechanism was proved to be that manganese was combined with sulfonic acid group. Several crucial parameters such as temperature, phosphoric acid content and resin dose were studied to optimize adsorption efficiency. Through optimization, removal percentage and sorption capacity of manganese reached 53.12 wt%, 28.34 mg·g^{-1} , respectively. Pseudo-2nd-order kinetic model simulated kinetics data best and the activation energy was evaluated as 6.34 kJ·mol^{-1} for the sorption reaction of manganese. In addition, the global adsorption rate was first controlled by film diffusion process and second determined by pore diffusion process. It was found that the resin could adsorb up to 50.24 mg·g^{-1} for manganese. Equilibrium studies showed that Toth adsorption isotherm model fitted best, followed by Temkin and Langmuir adsorption isotherm models. Thermodynamic analysis showed that manganese adsorption was an endothermic process with enhanced randomness and spontaneity.*

Keywords: *manganese, ion exchange, phosphoric acid, kinetics, isotherm, thermodynamics.*

Introduction. Phosphoric acid is a kind of basic chemical feedstock, which is extensively used in numerous industrial categories such as chemical fertilizers, detergents, food additives, electronic, medicine, beverages and so on [1–3]. Currently, phosphoric acid is produced industrially in two main ways, including thermal and wet methods. The thermal method technique is comprised of the combustion oxidation of yellow phosphorus and hydration absorption of phosphorus pentoxide, which although obtain highly purified phosphoric acid, it consumes much more energy than that of wet method [4]. In addition, the wet method is more environmentally friendly than the former. Wet method primarily decomposes phosphate rock with inorganic acid [3], and then separates the insoluble solids from the liquid phase. Therein, sulfuric acid route is used most widely because of its lower cost and simple operation. For another, with the sharp consumption of high-grade phosphate rock, mid-and-low grade phosphate rock will be mined more widely and intensely [5]. In recent years, most proportion of industrial phosphoric acid was manufactured by wet process [6]. However, undesired impurities in the phosphate rock, such as Fe, Mg, Al, Mn and some other solid and organic matters are leached out together with phosphorus

unavoidably [1,2], which will cause a battery of striking undesirable influence to the phosphoric acid purification and subsequent phosphorus based merchandise [7]. For instance, excess content of metal will: (1) reduce the concentration of solubilized phosphors; (2) lead to serious scaling in the pipes and equipment when enrichment [4]; (3) bring about more transportation cost due to the increasing viscosity of phosphoric acid; (4) result in the generation of sludge in the wet-process phosphoric acid, which may bring about blockage of pipeline; (5) cause the caking of chemical fertilizer, which is harmful to carriage, storage and application of fertilizer, (6) and so on. In addition, it has to mention that various metallic ions may accumulate in soils and permeate into underground and surface water through the intermediary of phosphate fertilizer [1]. The excess uptake of metallic ions by crop would inevitably lead to the increasing metal level of food and animals. As most metal elements, such as manganese, are not biodegradable, and the degradation ability of living organisms are limited, excess metal will gradually gather in the living organisms, which eventually caused various diseases and disorders to human health [8,9]. Therefore, wet-process phosphoric acid necessarily needs purification before subsequent applications. Various purification methods could be used in the impurity removing of wet-process phosphoric acid, including chemical precipitation [10,11], solvent extraction [12,13], crystallization [14,15] and ion exchange [16–20]. In these ways, ion exchange method has a great many satisfactory advantages, containing environment friendly, simple operation, financial efficiency and higher selectivity, and it has been widely used in the decontamination of wet-process phosphoric acid as well as some other aqueous systems [19,20]. For instance, in Qiu's investigation on the magnesium adsorption from phosphoric acid, the removal percentage was about 87 wt% [16]. Tang et al. investigated aluminum adsorption behavior in phosphoric acid solution system, and the adsorption process of aluminum accorded with pseudo-2nd-order kinetics model [17]. In Leng's study, the holistic reaction rate of adsorption process was determined by pore diffusion. At present, most researches concentrate on the removal of iron, aluminum, and magnesium of wet-process phosphoric acid, while there were little references about the elimination of manganese from wetprocess phosphoric acid. However, certain phosphate rock was of high manganese content, such as reddingite, eosphorite and manganese apatite. Through the direct-reverse flotation of phosphate rocks in advance, although phosphate concentrate with lower manganese content can be obtained [21], the manganese content of wet process phosphoric acid produced by phosphate concentrate was still not qualified. In addition, through literature search, it was found that few references were concerned with the manganese removal from phosphoric acid solution. Huang et al. employed self-developed extractant P1 to directly extract manganese from phosphoric acid, and the experiment results showed that the single-stage extraction percentage of extractant P1 for manganese was about 35% when the organic/aqueous phase ratio equaled 3:1. M.I. Amin et al. used several aliphatic alcohols to directly extract phosphoric acid from wet process acid to obtain high grade phosphoric acid. After three-stage counter current extraction, the manganese content decreased from 1860.0 $mg \cdot L^{-1}$ in crude phosphoric acid to 2.3 $mg \cdot L^{-1}$, or lower, in refined phosphoric acid. Motivated by the knowledge absence, this paper employed an ion exchange resin with strong acidity called Sinco-430 to separate manganese ion from phosphoric acid solution. Firstly, the influence of resin dosage, agitation speed, temperature, phosphoric acid content and mass ratio of resin to solution (hereafter referred to as S/L) on the sorption efficiency was studied systematically. In addition, adsorption mechanism and kinetics of manganese adsorption from phosphoric acid

was investigated. Finally, adsorption equilibrium, isotherm as well as thermodynamics of manganese removal process was explored minutely.

2. Materials and Methods

2.1. Materials The main properties of the cation exchange resin with strong acidity and polystyrene skeleton employed in this experiment was listed in Table 1. It was purchased from Aidiya Technology Co., Ltd. (Hubei, China). The stock solution was the compound of deionized water, $MnSO_4 \cdot H_2O$ powder and phosphoric acid, and the content of manganese was determined by ICP-AES. Deionized water and 5 wt% sulfuric acid were used to serve as pH regulator and regenerate the resin, respectively. In the previous research, the total exchange capacity of Sinco-430 had been measured. Compared with other resins, the employed resin in this paper has a larger exchange capacity, for example, the exchange capacity of IR-120, D113, Dowex 50 W-X8 [27], D001, and D152 were 5 mmol·g^{-1} , 0.02 mmol·g^{-1} , 4.8 mmol·g^{-1} , 4.50

Table 1

The properties of the cation exchange resin Sinco-430 [18]

Resin	Sinco-430
Functional group	—SO_3H
Ionic form	Na^+
Total exchange capacity/mmol·g^{-1}	5.18
Pore volume/ml·g^{-1}	0.0602
Specific surface area/m^2 ·g^{-1}	8.91
Free water content/wt%	55.31*
Average pore diameter/nm	27.02

mmol·g^{-1} , and 3.38 mmol·g^{-1} , respectively. Larger exchange capacity means more potential to purify the phosphoric acid solution.

2.2. Methods

2.2.1. Adsorption kinetics

The stock synthesis solution (fixed at about 400 g) and resin were added to a glass vessel at a certain mass ratio, whose height and diameter were 9.5 cm and 7.5 cm. Then the mixture was stirred at 400 rpm and the batch reactor was kept at preset temperature all the time. In order to study adsorption kinetics, three 20 μl liquid phase samples was simultaneously extracted at a certain time lag within thirty minutes to determine manganese content, and the mean manganese content of three sample was employed in this paper. The relative density of stock synthesis solution with 41.41 wt% phosphoric acid was about 1.26, which meant that its volume was roughly 317.46 ml. In addition, as you can see in our article, a total of 54 samples were taken for each experiment run, i.e., the total volume of samples accounts less than 0.34% of the whole volume of solution, which exert little impact on the entire experimental system. The adsorption amount of unit mass resin and removal percentage can be obtained by:

$$Q_t = \frac{(C_0 - C_t)V}{\mathrm{m}} \quad (1)$$

$$E_t = \frac{(C_0 - C_t)}{C_0} * 100 \quad (2)$$

where C_0 was manganese content at initial time, mg·L^{-1} ; Ct was the content of manganese at any time t, mg·L^{-1} ; m is the mass of resin, g; V is the volume of the aqueous solution, L; Qt is the adsorption amount of unit mass resin, mg·g^{-1} ; and Et is the adsorption percentage of manganese, %.

2.2.2. Adsorption isotherm

The experimental method of sorption isotherm was similar to adsorption kinetics. However, in the study of sorption isotherm, only the supernatant after equilibrium was analyzed for its manganese content. In order to obtain equilibrium data of this adsorbate/adsorbent system, stock solution containing various initial manganese content ranged from 0.05 wt% to 1.00 wt% (590 to 12,780 $mg \cdot L^{-1}$) was prepared. In addition, the mass of stock solution was fixed at about 400 g, H_3PO_4 content of the stock solution was set as 27.61 wt%, and S/L was fixed at 0.15. Each concentration of stock solution was performed at 20, 35 and 50 °C, respectively. Adsorption isotherm experiments were carried out with 400 $r \cdot min^{-1}$ of stirring rate for 1 h.

3. Results and Discussion

3.1. Adsorption mechanism analysis

3.1.1. FT-IR spectroscopy

Fig. 1 displayed the FT-IR spectroscopy of origin resin and the resin exchanged with manganese. The small band at 1126 cm^{-1} denoted the stretching vibration of S—O bonds, and the peak located in 1005 cm^{-1} was ascribed to stretching vibration of S==O bonds [18,30].

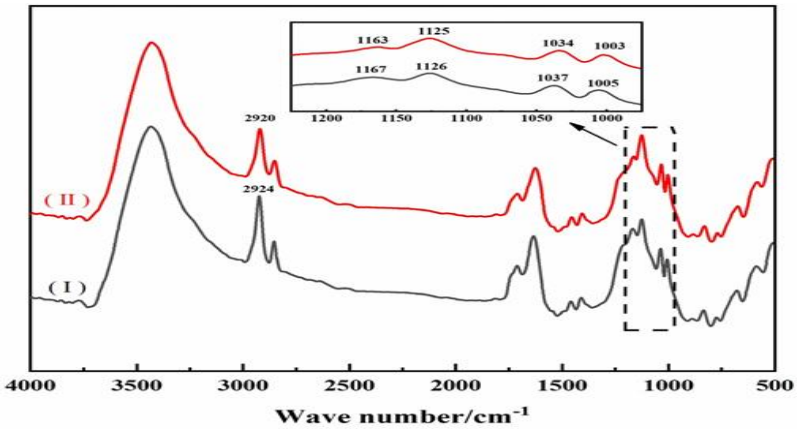

Fig. 1. FT-IR spectrum of resin before and after manganese sorption (I-before sorption, II-after sorption).

The infrared spectra peaks observed at 2920 cm^{-1} and 2924 cm^{-1} were due to the stretching vibration O—H bonds. In addition, the band from 1163 cm^{-1} to 1167 cm^{-1} showed the presence of —SO_3H in this kind of resin. The absorption peak around 1037 cm^{-1} was associated with P—O bonds [32]. In addition, it was found that the peaks at 1167, 1126, 1037, and 1005 cm^{-1} tended to move in the direction of low wave number, i.e., manganese adsorption caused red shift of sulfonic group, which might be due to the fact that the combination of manganese ions and sulfonic group reduced the electron effect [33]. According to the analysis above, it was clear that the sorption of manganese was chemical process and sulfonic group was the functional group of this resin. 3.1.2. XPS characterization Fig. 2 (a) presented the wide XPS spectrum of the resin before adsorption, and the main element was C, O, N and S. There was just a sort of binding energy (168.46 eV) for S 2p as shown in Fig. 2 (c), which was due to the function group —SO_3H. Fig. 2 (d) showed that O 1 s had two types of binding energy, around at 531.74 and 533.44 eV, respectively. The reason of this result was that O 1 s located in the different positions of molecular structure, i.e., there were two different chemical bonds for O 1 s (S==O, S—O). Furthermore, the peak area of S==O was about twice that of S—O. The resin after manganese adsorption was also characterized by XPS, and its full spectrum was depicted in Fig. 3 (a), which indicated that manganese participated in the adsorption reaction with resin indeed. However, the combination of

manganese and sulfonic acid group had altered the chemical environment of S and O. The peaks for S 2p at 169.25 eV and 168.07 eV in Fig. 3 (c) revealed the existence of Mn— SO_3 and —SO_3H in the resin, respectively. It was found that there were three different peaks for O 1 s, the binding energy of these peaks were 533.70 (Mn—O—S), 532.64 (S—O) and 531.64 eV (S==O), respectively. Thereinto, the peak at 533.70 eV proved the exchange of manganese and proton. 3.1.3. Reaction mechanism The mechanism of the reaction between manganese ion and sulfonic acid group is mostly electrostatic interaction, which could be elucidated by Donnan membrane equilibrium theory [36]. Ion-exchange resins are generally composed of polymer chains, and fixed charged groups attached to the chain skeletons. These fixed charges that are bound to the resin phase are the functional groups of the resin, and the mobile charges possessing a sign of charge that is opposite to the fixed charges, are called the counter-ions.

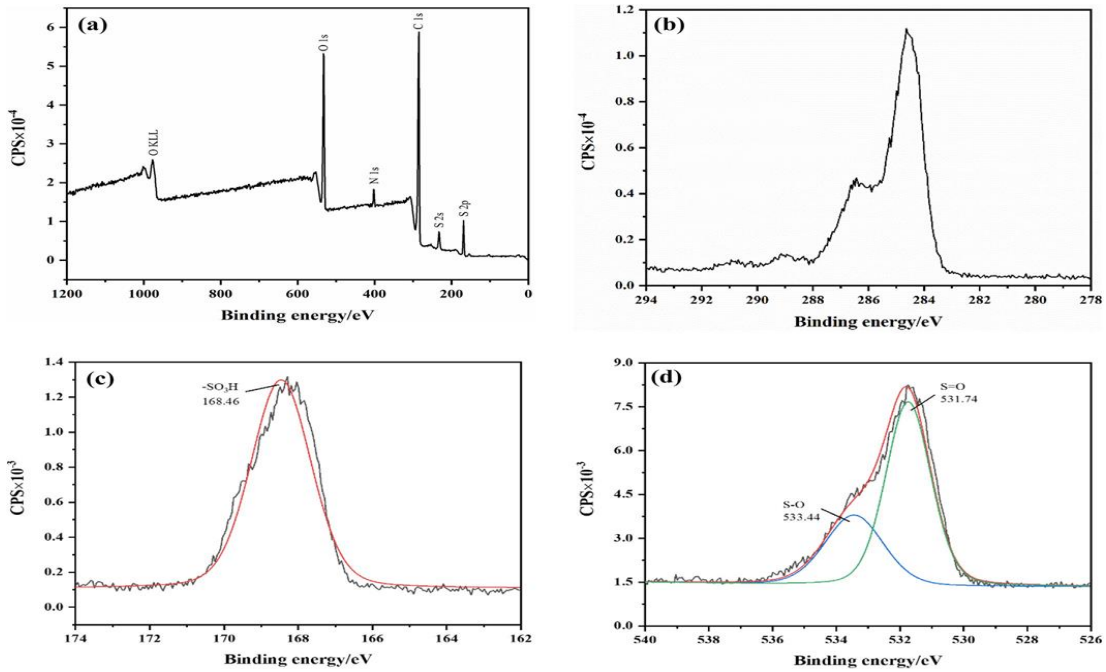

Fig. 2. XPS spectra of resin before manganese sorption: (a) wide, (b) C 1 s, (c) S 2p, (d) O 1 s.

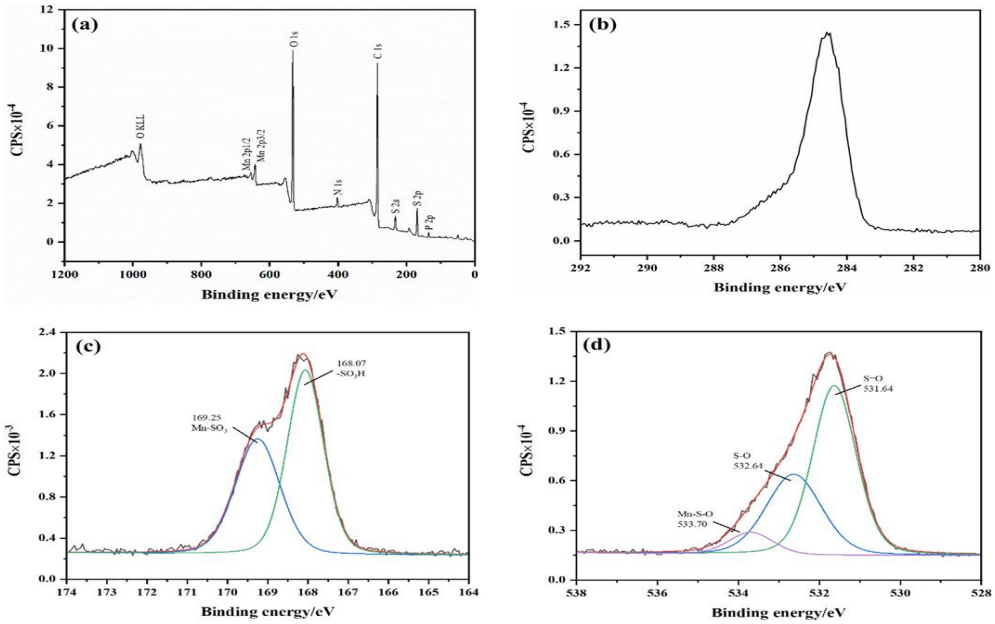

Fig. 3. XPS spectra of resin after manganese sorption: (a) wide, (b) C 1 s, (c) S 2p, (d)O 1 s.

Meanwhile, the mobile charges that have the same sign as the fixed charges are called the co-ions. In the ion-exchange resin, solute-matrix interactions (van der Waals forces), ion-dipole interactions (polarization), and ion-solvent interactions (hydration) are much weaker than electrostatic interactions between resin and ions, their contribution to ion-exchange behavior were usually not considered. In addition, the electrostatic interactions between fixed charges and mobile charges are long-range interaction, hence the resin phase is usually considered as a homogeneous phase. For the ion-exchange system in this paper, the fixed charges of the resin are sulfonic acid groups. Counter-ions present in the phosphoric acid, including Mn^{2+} and other counter-ions, can exchange with the H^+ previously in the matrix of the resins. However, co-ions in the phosphoric acid ($SO4^{2-}$, $H_2PO_4^-$, HPO_4^{2-}, PO_4^{3-}) are excluded from the resin because of the Donnan potential at the resin-solution interface [40]. Because sulfonic acid groups are preferentially bonded to bivalent Mn^{2+} than the monovalent H^+, the Mn^{2+} ions are therefore enriched in the resin phase, leading to the purification of the phosphoric acid solution.

3.2. Kinetics studies

3.2.1. Preliminary study on manganese sorption efficiency for Sinco430 resin.

In this preliminary test, the mass of the resin was set as the only variable to study its influence on the adsorption percentage of manganese. As presented in Fig. 4, adsorption percentage rose from 12% to 80%, which was accompanied by resin dosage raising from 2.5 g to 30 g. However, adsorption capacity of unit mass resin was reduced by 44% from 41 $mg \cdot g^{-1}$ correspondingly. Both removal percentage and adsorption capacity of unit mass resin were important parameters, therefore the mass ratio of 15 g resin to 100 g aqueous solution was employed without variation in the following experiment, studying the other factors that influence sorption behavior.

3.2.2. Influence of stirring rate on the adsorption rate of manganese.

In order to eliminate the external diffusion of bulk liquid phase, several experiments with various agitation speeds were carried out for 5 min, and the results were shown in Fig. 5. Apparently, external diffusion was nearly removed when the revolving speed was over 200 $r \cdot min^{-1}$. Moreover, the removal percentage gained sharp growth during 0 and 200 $r \cdot min^{-1}$, which meant that manganese sorption might be controlled by diffusion process.

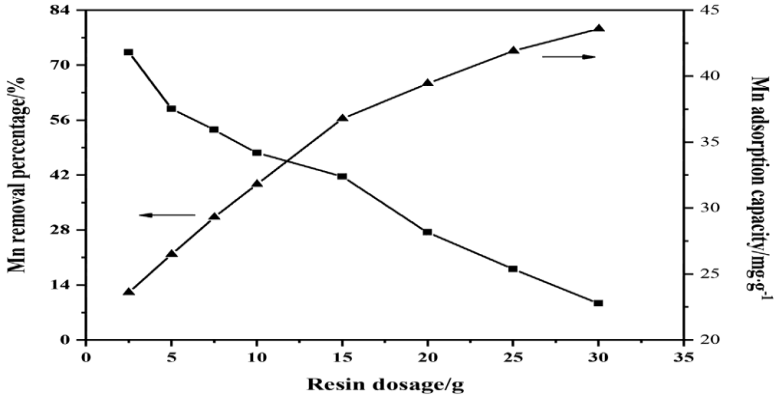

Fig. 4. Preliminary investigation on manganese adsorption efficiency with increasing resin dosage (aqueous solution mass and manganese content was fixed at 100 g and 0.8 wt%, respectively).

Unless otherwise specified, stirring rate of all the following experiments were set as 400 $r \cdot min^{-1}$, and there was no need to discuss the effect of revolving speed on reaction rate of manganese adsorption. 3.2.3. Influence of temperature on manganese removal efficiency Fig. 6

described the variation of manganese concentration and removal percentage under different temperature. H_3PO_4 concentration was 27.61 wt%, mass ratio of solid to liquid phase was 0.15 and original manganese content was 0.8 wt%. As shown in Fig. 6, the manganese content in solution at equilibrium state was 0.424 wt%, 0.411 wt%, 0.392 wt % and 0.382 wt% for 20, 35, 50 and 65 °C, respectively. This was because rising temperature caused reaction equilibrium moved in the direction of adsorption, and adsorption reaction might be a heat-absorbing process.

3.2.4. Influence of H_3PO_4 content on manganese removal percentage

The effect of H_3PO_4 content on the adsorption efficiency of manganese was presented in Fig. 7. Adsorption temperature was 35 °C, manganese content in solution at initial moment was 0.8 wt%, and mass ratio of resin to solution was 0.15. From the beginning of adsorption reaction, the reaction equilibrium was reached after 18 min.

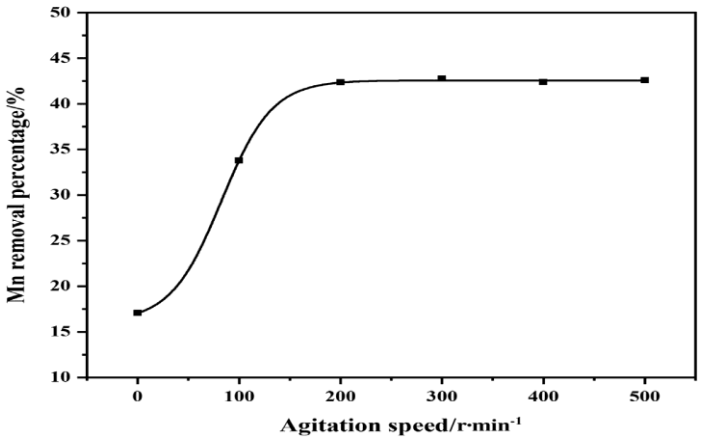

Figure 5

And manganese content in solution at equilibrium state was 0.26 wt%, 0.29 wt%, 0.34 wt%, 0.39 wt% and 0.43 wt% at increasing phosphoric acid content, respectively. This changing sorption behavior may attribute to the fact that increasing phosphoric acid content released a greater number of protons, which deactivated exchange sites loaded with sulfonic acid group.

3.2.5. Influence of mass ratio of resin to solution on the removal percentage of manganese.

Fig. 8 described manganese content and removal percentage under different mass ratios of resin to solution. Initial manganese content, phosphoric acid content and temperature were kept at 0.8 wt%, 27.61 wt% and 35 °C, respectively. The manganese content in solution at equilibrium state was 0.64 wt%, 0.38 wt% and 0.22 wt% at the increasing mass ratios, respectively. Moreover, sorption capacity of unit mass resin was 23.40 $mg \cdot g^{-1}$, 28.38 $mg \cdot g^{-1}$ and 32.14 $mg \cdot g^{-1}$ for the incremental mass ratio, respectively. These suggested that although raising mass ratio contributes to increasing adsorption efficiency but it also reduced the sorption amount per unit resin in the same time. Through a series of experiments mentioned above, optimized technological parameters such as agitation speed, temperature, phosphoric acid content and mass ratio of resin to solution was 400 $r \cdot min^{-1}$, 35 °C, 27.61 wt% and 0.15.

3.3. Kinetics studies

3.3.1. Adsorption kinetics

Adsorption kinetics models were generally used to build relationship between sorption amount of adsorbate and time, and the models were also very significant to the process design of aqueous system purification. To figure out the connection between manganese sorption amount and reaction time, pseudo-1st-order and pseudo-2nd-order kinetics models were employed, and their equations were mathematically given as below in order:

$$\ln (Q_e - Q_t) = \ln Q_e - k_1 t$$

$$\frac{t}{Q_t} = \frac{1}{Q_2 Q_e} + \frac{t}{Q_e}$$

where Qt is adsorption capacity at time t, $mg \cdot g^{-1}$; Q_e is adsorption capacity at equilibrium, $mg \cdot g^{-1}$; k_1 and k_2 were the reaction rate constants of pseudo-1st-order and pseudo-2nd-order kinetics model, respectively. In Table 2, the values of R_2 (correlation coefficient) of the first-order model were all over 0.88, but there was a big deviation between its equilibrium adsorption capacity (Q_e,1) and experiment value (Q_e,exp). However, the corresponding coefficients of pseudo-2nd-order kinetics model were all greater than 0.999, moreover the equilibrium adsorption capacity of pseudo-2nd-order model (Q_e,2) was almost identical to Q_e, exp, which indicated that pseudo-2nd-order model could satisfactorily depict manganese sorption kinetics. The activation energy (Ea) of adsorption reaction could be obtained by using Arrhenius equation:

$$\ln k_2 = \ln A - E_a/RT$$

For manganese sorption reaction, its activation energy was ascertained as 6.34 kJ·mol−1 by using the slope value of $\ln k_2$ versus 1/T in the Fig. 9, which manifested that adsorption process rate could be determined by film or pore diffusion process, while for adsorption reaction with activation energy above 50 $kJ \cdot mol^{-1}$, its entire adsorption rate was determined by chemical reaction process.

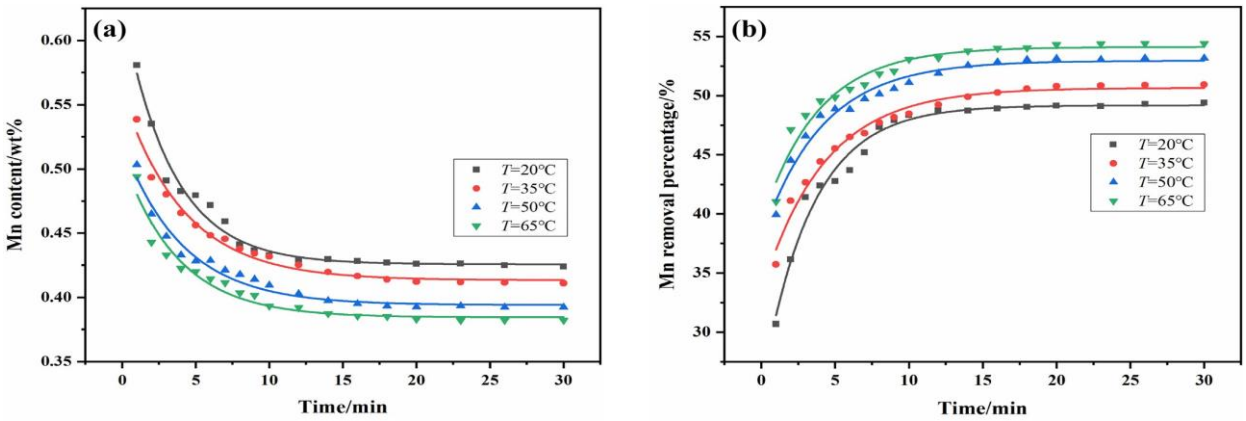

Fig. 6. The influence of temperature on the manganese sorption capacity.

Conclusions

In this paper, we triumphantly conducted a systematic investigation on the adsorption behavior of manganese from phosphoric acid using Sinco-430 cation-exchange resin. The results of FT-IR and XPS proved sorption mechanism to be that manganese was combined with — SO_3H. Phosphoric acid content and the mass proportion of resin to solution showed significant impact on the manganese adsorption efficiency, while temperature exerted little positive influence. Kinetics study indicated that manganese sorption process could be better represented by pseudo-2nd-order kinetics model, and the activation energy of adsorption reaction was 6.34 $kJ \cdot mol^{-1}$. The application result of diffusion models showed that the rate-determining step of manganese sorption process was film and pore diffusion process in succession. Isotherm studies showed that the adsorption behavior of the resin followed Toth isotherm model best, and the experimental value of maximum manganese adsorption capacity was 50.24 $mg \cdot g^{-1}$, which was almost the same as the calculated value of Toth isotherm model. Manganese sorption process was an endothermic process with entropy increase and spontaneity. The obtained conclusions above indicated that Sinco430 could be considered as a satisfactory cation exchange resin for the removal of manganese from phosphoric acid.

REFERENCES

1. S. Kouzbour, B. Gourich, F. Gros, C. Vial, F. Allam, Y. Stiriba, Comparative analysis of industrial processes for cadmium removal from phosphoric acid: A review, Hydrometallurgy. 188 (2019) 222–247.
2. R. Kijkowska, D. Pawlowska-Kozinska, Z. Kowalski, M. Jodko, Z. Wzorek, Wet-process phosphoric acid obtained from Kola apatite. Purification from sulphates, fluorine, and metals, Sep. Purif. Technol. 28 (2002) 197–205.
3. Benjamín Valdez Salas, Michael Schorr Wiener, J.R.S. Martinez, Phosphoric Acid Industry: Problems and Solutions, Phosphoric Acid Industry - Problems and Solutions, IntechOpen (2017)https://doi.org/10.5772/intechopen.70031https://www. intechopen.com/books/phosphoric-acid-industry-problems-and-solutions/phosphoric-acid-industry-problems-and-solutions.
4. M.B. Hocking, Handbook of Chemical Technology and Pollution Control, Third edition Academic Press, San Diego, 2005.
5. S. Samreen, S. Kausar, Phosphorus Fertilizer: The Original and Commercial Sources, Phosphorus - Recovery and Recycling, IntechOpen, 2019https://www.intechopen. com/books/phosphorus-recovery-and-recycling/phosphorus-fertilizer-the-originaland-commercial-sources.
6. J. Luo, J. Li, Y. Jin, Y. Zhang, D. Zheng, Study on Mg^{2+} removal from ammonium dihydrogen phosphate solution by predispersed solvent extraction, Ind. Eng. Chem. Res. 48 (2009) 2056–2060.
7. L. Khamar, M.E. Guendouzi, M. Amalhay, M.a.E. Alaoui, A. Rifai, J. Faridi, M. Azaroual, Evolution of soluble impurities concentrations in industrial phosphoric acid during the operations of desupersaturation, Proc. Eng. 83 (2014) 243–249.
8. S.P. Ramoju, D.R. Mattison, B. Milton, D. Mcgough, N. Shilnikova, H.J. Clewell, M. Yoon, M.D. Taylor, D. Krewski, M.E. Andersen, The application of PBPK models in estimating human brain tissue manganese concentrations, Neurotoxicology. 58 (2017) 226–237.
9. J.A. Roth, Homeostatic and toxic mechanisms regulating manganese uptake, retention, and elimination, Biol. Res. 39 (2006) 45–57.
10. H.M. Abdel-Ghafar, E.A. Abdel-Aal, M.a.M. Ibrahim, H. El-Shall, A.K. Ismail, Purification of high iron wet-process phosphoric acid via oxalate precipitation method, Hydrometallurgy 184 (2019) 1–8.
11. S. Wu, L. Zhao, L. Wang, X. Huang, Y. Zhang, Z. Feng, D. Cui, Simultaneous recovery of rare earth elements and phosphorus from phosphate rock by phosphoric acid leaching and selective precipitation: towards green process, J. Rare Earths 37 (2019) 652–658.
12. Y. Jin, Y. Ma, Y. Weng, X. Jia, J. Li, Solvent extraction of Fe3+ from the hydrochloric acid route phosphoric acid by D2EHPA in kerosene, J. Ind. Eng. Chem. 20 (2014) 3446–3452.

A. Hannachi, D. Habaili, C. Chtara, A. Ratel, Purification of wet process phosphoric acid by solvent extraction with TBP and MIBK mixtures, Sep. Purif. Technol. 55 (2007) 212–216.

13. L.-P. Dang, H.-Y. Wei, Effects of ionic impurities on the crystal morphology of phosphoric acid hemihydrate, Chem. Eng. Res. Des. 88 (2010) 1372–1376.
14. L. Dang, H. Wei, Z. Zhu, J. Wang, The influence of impurities on phosphoric acid hemihydrate crystallization, J. Cryst. Growth 307 (2007) 104–111.